Available online at www.sciencedirect.com
ScienceDirect
Trans. Nonferrous Met. Soc. China 32(2022) 739−749
Transactions of Nonferrous Metals Society of China
www.tnmsc.cn

Preparation of semi-solid 6061 aluminum alloy slurry by serpentine channel pouring

Nai-yong LI, Wei-min MAO, Xiao-xin GENG

School of Materials Science and Engineering, University of Science and Technology Beijing, Beijing 100083, China

Received 3 March 2021; accepted 3 November 2021

Abstract: The semi-solid 6061 aluminum alloy slurry was prepared by a serpentine channel pouring process. The effects of pouring temperature, bend number and bend diameter on the microstructures were investigated. Microstructural evolution mechanism of the semi-solid slurry during the pouring process was also analyzed. The results show that the grain is refined and the grain roundness is improved by controlling the pouring temperature close to the liquidus temperature, and the nucleation rate of primary α(Al) grains is effectively increased via increasing the bend number and decreasing the bend diameter. The primary grains are not only formed directly from the alloy melt via chilling nucleation and heterogeneous nucleation, but also evolved from the fractured dendrite fragments. Meanwhile, the heat exchange between the melt and the serpentine channel is increased by the "self-stirring" effect in the melt, which also promotes the refinement and spheroidization of primary α(Al) grains.

Key words: 6061 aluminum alloy; semi-solid slurry; serpentine channel; microstructural evolution

1 Introduction

6061 aluminum alloy is widely used in transportation, civil engineering and aerospace fields due to its good plasticity, corrosion resistance, weldability and heat treatment strengthening [1−3]. However, it is unsuitable for casting some thin-walled parts because of its tendency of hot cracking and coarse dendritic structure during traditional permanent casting process. More importantly, the hot cracking is inevitable and hard to eliminate, and it has adverse effect on the mechanical properties of components. Therefore, it is crucial to improve the structure and properties of aluminum alloy castings [4]. Nowadays, researchers mainly adopt methods such as rapid cooling, vibration and adding nucleating agents to improve the microstructure of ingots [5−7]. But, these processes may be complicated and have little effect on reducing the tendency of hot cracking.

In recent years, semi-solid metal (SSM) forming has received more and more attention as a promising technology to improve the structures and properties of aluminum alloy castings [8]. Compared with traditional permanent casting process, it has low solidification shrinkage and is possible to reduce the tendency of hot cracking of 6061 aluminum alloy castings. At present, a large amount of research on SSM technology has been focused on the aluminum alloys and magnesium alloys. JIANG and WANG [9] reported using the ultrasonic-assisted semisolid stirring to prepare a spheroidized semi-solid slurry of SiC/7075 aluminum matrix composite with good mechanical properties. CHANG et al [10] studied the semi-solid rheology of magnesium alloys and explained the formation mechanism of non-dendritic structure during the preparation of rheological slurry. KUMAR et al [11] and MATHEW et al [12] prepared a non-dendritic feedstock for thixoforming by a cooling slope casting

Corresponding author: Wei-min MAO, Tel: +86-13911069562, E-mail: mao_wm@ustb.edu.cn
DOI: 10.1016/S1003-6326(22)65829-1

technique and reported the effect of semi-solid forging on microstructure and mechanical properties.

An appropriate method of slurry preparation is vital to the SSM process. In recent years, researchers have proposed a variety of semi-solid slurry preparation processes. WANG et al [13] prepared the semi-solid Mg−Gd−Zn alloy slurry with non-dendritic structure by a low-frequency electromagnetic stirring method. FAN et al [14] prepared the semi-solid billets of AZ80−0.2Y−0.15Ca magnesium alloy by a strain-induced melt activation (SIMA) process. QI et al [15] prepared the high-quality semi-solid slurries of aluminum and magnesium alloys by a distributary-confluence channel (DCC) process. Although many other slurry preparation processes can also well obtain non-dendritic microstructure, the problems of high cost and complicated operation still exist.

In order to solve the above-mentioned difficulty, a serpentine channel pouring (SCP) process with simple operation, low cost and high efficiency was proposed to prepare high-quality semi-solid slurry several years ago [16,17]. The spherical primary grains in slurry were formed by the chilling effect as well as the heterogeneous nucleation on the inner channel surface during the pouring process. In addition, the uniformity of temperature field and concentration field was promoted by the "self-stirring" effect in the melt, so more primary grains were survived. Up to now, research on SCP of 6061 aluminum alloy was reported little. Therefore, the SCP process will be applied to this material in the present research. The microstructures of slurry were significantly affected by the pouring temperature and the serpentine channel characteristic parameters. In order to clarify the influence of pouring temperature, bend number and bend diameter on slurry preparation, the microstructures of semi-solid 6061 slurry prepared by the SCP process with different parameters were investigated. Finally, the microstructural evolution mechanism of the semi-solid slurry during the pouring process was also analyzed.

2 Experimental

2.1 Materials

The commercial 6061 aluminum alloy was selected in this study, whose chemical composition is given in Table 1.

For determining the SCP process parameters, the differential scanning calorimetry (DSC) analysis of 6061 aluminum alloy was carried out by a NETZSCHSTA409C/CD differential scanning calorimeter. Figure 1 presents the DSC curve of the alloy, depicting the solidus and liquidus temperatures of 597 and 646 °C, respectively.

Table 1 Chemical composition of 6061 aluminum alloy (wt.%)

Si	Mg	Cu	Cr	Ti	Fe	Zn	Mn	Al
0.60	1.00	0.30	0.20	0.10	≤0.20	≤0.25	≤0.15	Bal.

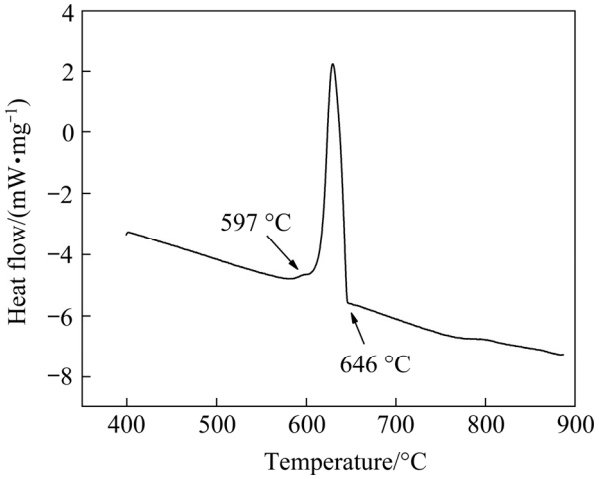

Fig. 1 DSC curve of 6061 aluminum alloy

2.2 Methods

The schematic diagram of the SCP process is shown in Fig. 2. The 6061 aluminum alloy ingot was firstly melted with a crucible resistance furnace at 800 °C. After the alloy was completely melted into a liquid, it was degassed and refined for 10 min through a graphite lance by Ar. Then, the melt was transferred out of the resistance furnace, and the slag was removed. The temperature of the melt was measured by a Ni−Cr/Ni−Si thermocouple. Subsequently, the melt was cooled down to a preset pouring temperature and then poured into a graphitic serpentine channel to prepare semi-solid slurry. The SCP process parameters for the slurry preparation and characteristic size of slurry are listed in Table 2. Afterwards, the slurry was collected via a copper crucible. At the same time, the outlet temperature of the slurry was recorded. Finally, the copper collection crucible was quickly quenched in water to retain the semi-solid structure.

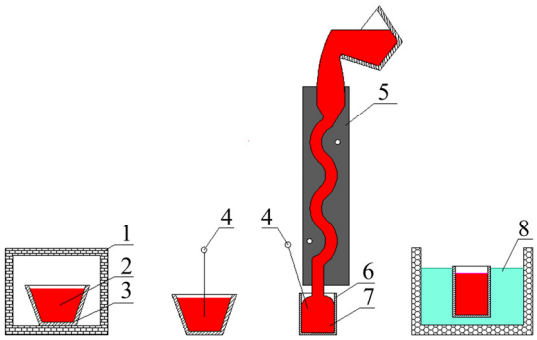

Fig. 2 Schematic diagram of SCP process: 1−Crucible resistance furnace; 2−6061 aluminum alloy melt; 3−Graphite crucible; 4−Thermocouple; 5−Serpentine channel mold; 6−Copper collection crucible; 7−Semi-solid slurry; 8−Cold water

The metallographic samples were cut from the center part of the slurry ingots. The samples were etched with a Keller reagent (1 mL HF + 1.5 mL HCl + 2.5 mL HNO_3 + 95 mL H_2O) after rough grinding, fine grinding and polishing. Subsequently, the microstructures of the samples were observed by a Neuphoto21 optical microscope (OM). The morphology of the solidified shell surface was observed via a ZEISS SUPRA40 scanning electron microscope (SEM). Furthermore, the average grain diameter and average shape factor of primary α(Al) grains were analyzed and calculated using professional image analysis software Image-Pro Plus. The calculation formulas are given in Eqs. (1) and (2) [18,19]:

$$D=\frac{1}{N}\sum_{i=1}^{N}\sqrt{4A/\pi} \tag{1}$$

$$F_s=N/\sum_{i=1}^{N}[P^2/(4\pi A)] \tag{2}$$

where D, F_s, A, N and P are the average grain diameter, average shape factor, area, number of grains and perimeter of the primary α(Al) grains, respectively. The average shape factor is used to characterize the roundness of primary grains, with the value close to 1 indicating high grain roundness.

3 Results

3.1 Microstructure

Figure 3 shows the typical microstructures of the 6061 aluminum alloy produced by the SCP process, in comparison with the same alloy prepared by a traditional permanent casting. This alloy mainly consists of α(Al) matrix and β-Mg_2Si phase [20]. As shown in Fig. 3(a), the conventional as-cast 6061 aluminum alloy exhibits a coarse and non-uniform microstructure. The bright regions are mainly primary α(Al) dendrites, and the gray lines are mainly eutectic structures formed by residual melt.

Table 2 presents that the outlet temperature of slurry is below the liquidus temperature, which indicates that a semi-solid slurry is obtained. The slight difference between the outlet temperatures is caused by the non-equilibrium solidification during the SCP process. Figures 3(b−i) show the microstructures of semi-solid slurry in different casting processes. As shown in Fig. 3(b), the primary α(Al) grains of semi-solid slurry are mainly composed of spherical, near-spherical and rose-like morphology. Obviously, the primary grains of semi-solid slurry are refined and spheroidized compared with the traditional as-cast ones.

Table 2 Process parameters and characteristic size of semi-solid slurry

Bend number	Bend diameter/mm	Pouring temperature/°C	Outlet temperature/°C	Average grain diameter/μm	Average shape factor
4	20	660	625	87.12±46.32	0.65±0.18
4	20	690	633	123.29±63.76	0.63±0.16
4	20	720	645	125.79±78.23	0.59±0.22
5	20	660	623	72.07±36.53	0.67±0.16
5	20	690	630	110.14±43.72	0.66±0.14
5	20	720	642	125.07±55.42	0.60±0.13
6	20	660	622	56.08±22.71	0.73±0.14
6	25	660	625	68.60±33.40	0.72±0.15

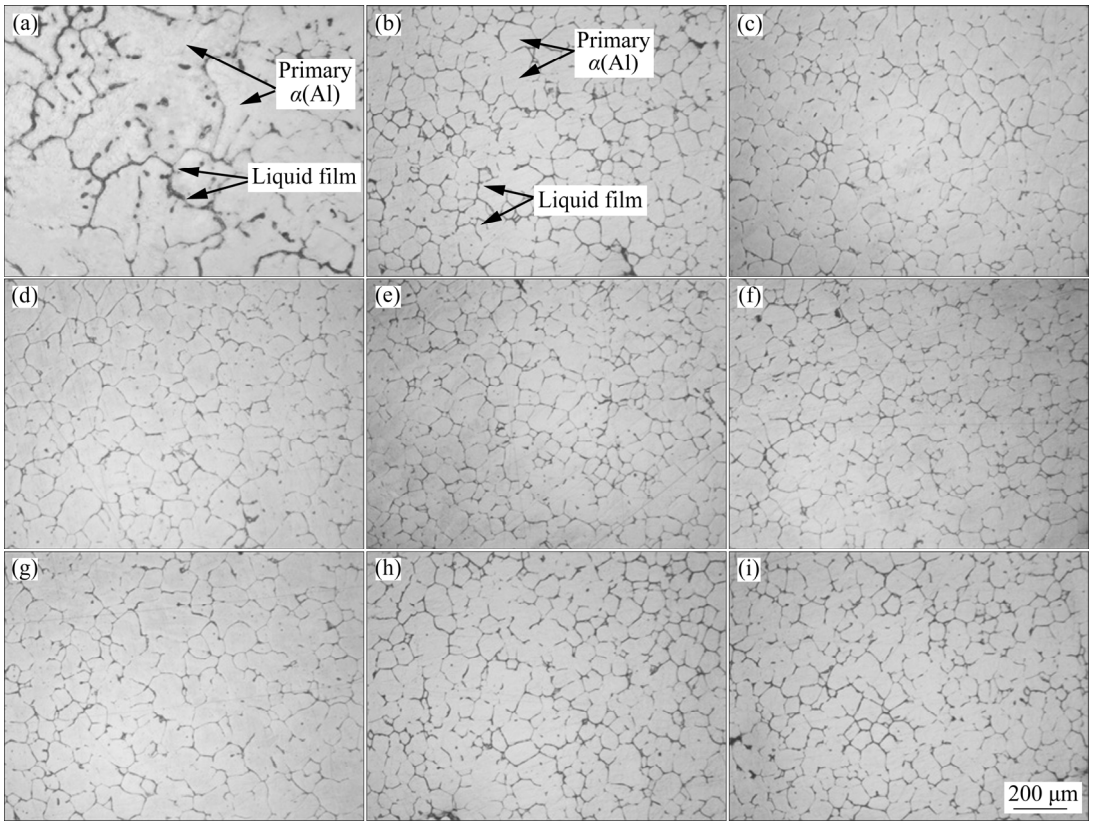

Fig. 3 Microstructures of traditional as-cast and semi-solid slurry: (a) Traditional permanent casting; (b) 4 bends, 20 mm, 660 °C; (c) 4 bends, 20 mm, 690 °C; (d) 4 bends, 20 mm, 720 °C; (e) 5 bends, 20 mm, 660 °C; (f) 5 bends, 20 mm, 690 °C; (g) 5 bends, 20 mm, 720 °C; (h) 6 bends, 20 mm, 660 °C; (i) 6 bends, 25 mm, 660 °C

3.2 Effects of pouring temperature on microstructure

The microstructures with bend diameter of 20 mm, bend number of 4 (Figs. 3(b−d)) and 5 (Figs. 3(e−g)) at different pouring temperatures are discussed. Figure 4 presents the size and distribution of primary α(Al) grains with different pouring temperatures. As seen in Figs. 4(a, b), with increasing pouring temperature from 660 to 720 °C, the average grain diameter with 4 bends gradually increases from (87.12±46.32) to (125.79±78.23) μm, while the average shape factor gradually decreases from 0.65±0.18 to 0.59±0.22. The average grain diameter with 5 bends gradually increases from (72.07±36.53) to (125.07±55.42) μm, while the average shape factor gradually decreases from 0.67±0.16 to 0.60±0.13. It can be seen from Figs. 4(c, d) that the grain diameter of primary α(Al) is mostly distributed in the range of 30−90 μm at 660 °C, 50−170 μm at 690 °C, and 50−190 μm at 720 °C, respectively. This indicates that controlling the pouring temperature close to the liquidus is beneficial to forming fine grains.

It can be concluded from the above results that the pouring temperature has an important effect on the slurry preparation. During the SCP process, the primary grains can nucleate rapidly due to the chilling effect of the channel wall after the melt is poured into the channel. At the same time, the channel wall surface acts as a substrate for heterogeneous nucleation, leading to a large number of primary grains. If the pouring temperature is higher, the chilling effect of the channel wall is weakened, and the thermal diffusion efficiency is lower. In addition, some fine nuclei are remelted in a high-temperature melt, which decreases the nucleation rate of primary grains. If the pouring temperature is lower, the chilling effect of the channel wall is stronger and the thermal diffusion efficiency is higher. Moreover, a larger supercooling is formed, which increases the nucleation rate of primary grains. However, if the pouring temperature is too low, the viscosity of the melt increases rapidly, and some solidified primary grains are easy to remain and gather on the channel wall surface, forming a residual solidified shell.

3.3 Effects of bend number on microstructure

The microstructures with bend diameter of 20 mm, pouring temperature of 660 °C and bend number of 4, 5, and 6, respectively, are studied, as shown in Fig. 5. Figures 5(a, b, c) correspond to the partial enlarged views of Figs. 3(b, e, h), respectively. It can be seen that most of the primary grains have spherical and near-spherical morphology.

Figure 6 shows the size and distribution of primary α(Al) grains with different bend numbers. As seen in Fig. 6(a), with increasing bend number from 4 to 6, the average grain diameter gradually decreases from (87.12±46.32) to (56.08±22.71) μm, while the average shape factor gradually increases from 0.65±0.18 to 0.73±0.14. As shown in Fig. 6(b), the distribution of primary grains with 4 bends and 5 bends are both mostly in the range of 30−90 μm, while that with 6 bends is mostly in the range of 50−110 μm. However, the relative frequency of 4 bends is larger than that of 5 bends and 6 bends when the grain diameter is above 120 μm. This indicates that the grain size of 4 bends is relatively larger.

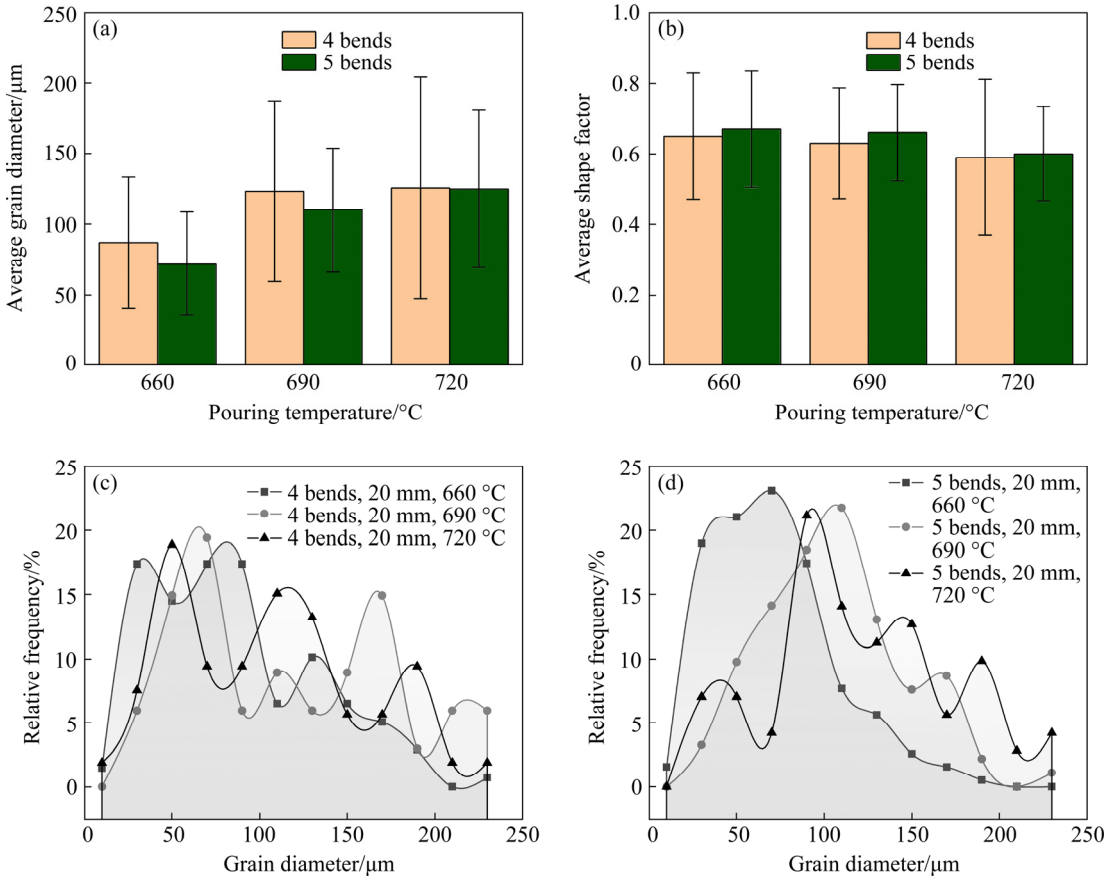

Fig. 4 Size and distribution of primary grains with different pouring temperatures: (a) Average grain diameter; (b) Average shape factor; (c) Relative frequency of 4 bends; (d) Relative frequency of 5 bends

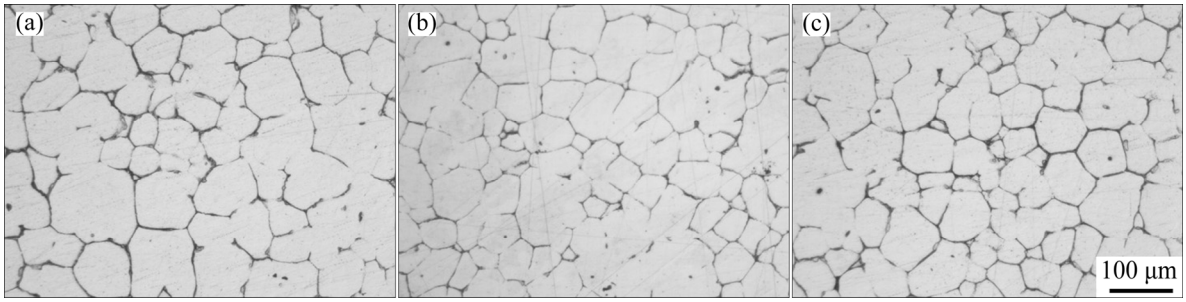

Fig. 5 Microstructures of semi-solid slurry with different bend numbers: (a) 4 bends, 20 mm, 660 °C; (b) 5 bends, 20 mm, 660 °C; (c) 6 bends, 20 mm, 660 °C

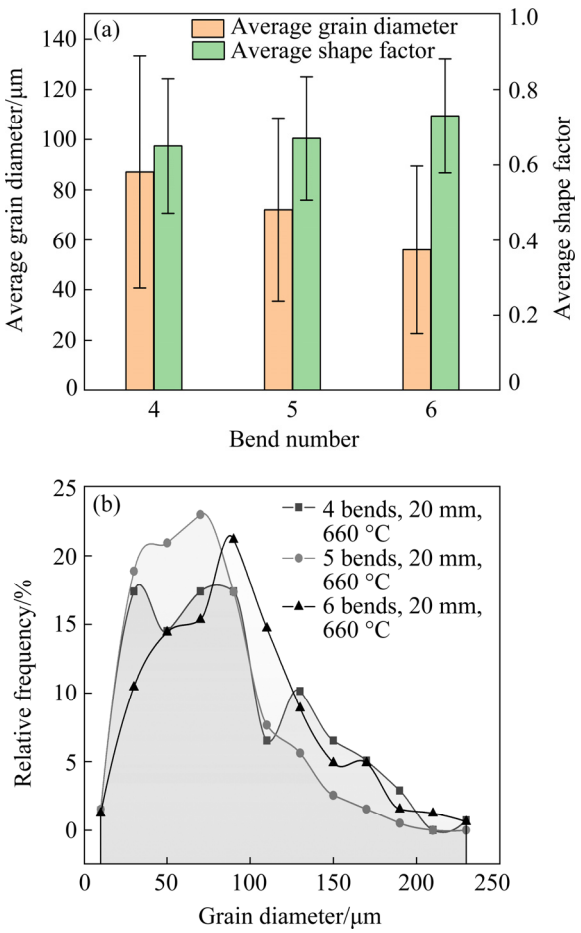

Fig. 6 Size and distribution of primary grains with different bend numbers: (a) Average grain diameter and average shape factor; (b) Relative frequency

It is clear that the bend number has a great influence on the size and roundness of primary α(Al) grains. During the SCP process, the effective contact area between the melt and the inner channel wall increases with increasing bend number, and the nucleation rate inside the channel is also increased. This indicates that the overheating and crystallization latent heat of the melt are more easily absorbed by the serpentine channel, resulting in a promotion of heterogeneous nucleation rate. Moreover, the displacement and shear direction of the melt are changed during the melt flows through each bend, resulting in "self-stirring" [21] in the melt. The "self-stirring" effect can not only strengthen the heat exchange between the melt and serpentine channel, but also reduce the temperature gradient and concentration gradient in the melt, leading to more free primary grains survived. More importantly, the uniformity of temperature field and concentration field in the melt is crucial to the refinement and spheroidization of primary grains, which also has a great effect on inhibiting the growth of dendrites.

3.4 Effects of bend diameter on microstructure

The microstructures with pouring temperature of 660 °C, bend number of 6 and bend diameter of 20 mm (Fig. 3(h)) and 25 mm (Fig. 3(i)) are analyzed, respectively. Figure 7 displays the size and distribution of the primary α(Al) grains with bend diameter of 20 and 25 mm. As seen in Fig. 7(a), with increasing bend diameter from 20 to 25 mm, the average grain diameter increases from (56.08±22.71) to (68.60±33.40) μm, while the average shape factor decreases from 0.73±0.14 to 0.72±0.15. As shown in Fig. 7(b), the highest relative frequencies for bend diameter of 20 and 25 mm appear at about 50 and 40 μm, respectively. However, the relative frequency with bend diameter of 20 mm is significantly higher than that of 25 mm in the range of 28−78 μm. In contrast, the relative

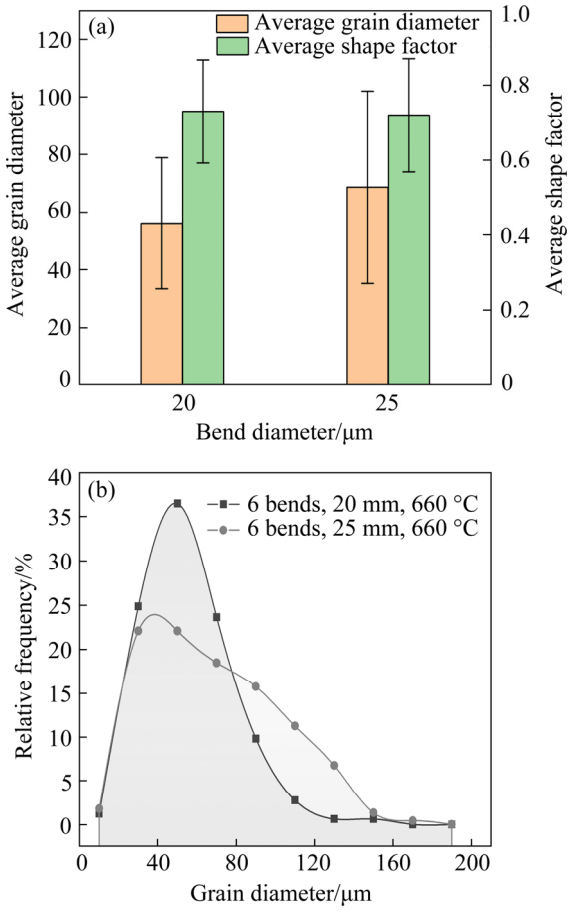

Fig. 7 Size and distribution of primary grains with bend diameter of 20 and 25 mm: (a) Average grain diameter and average shape factor; (b) Relative frequency

frequency with bend diameter of 25 mm is higher when the grain diameter is above 78 μm. This indicates that the grain size with bend diameter of 20 mm is finer and more uniform.

Figures 8(a, b) show the solidified shell with pouring temperature of 660 °C, bend number of 6 and bend diameter of 20 and 25 mm, respectively. The mass of solidified shell with bend diameter of 20 mm is relatively less than that of 25 mm, which can be attributed to the reduction of melt passing through the channel per unit time. In addition, the inner channel curvature increases with decreasing bend diameter, and the effective contact area increases between the melt and the inner channel wall, which promotes the heterogeneous nucleation. Moreover, the "self-stirring" effect in the melt is also strengthened, resulting in a relatively uniform temperature field and concentration field. It is obvious that the uniformity of the melt is beneficial to the spheroidization of primary grains.

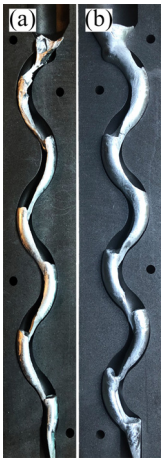

Fig. 8 Solidified shell with different bend diameters: (a) 6 bends, 20 mm, 660 °C; (b) 6 bends, 25 mm, 660 °C

4 Discussion

The semi-solid 6061 aluminum alloy slurry can be well prepared by the SCP process. After comprehensive analysis on the slurry preparation with different casting processes, the results indicate that the pouring temperature, bend number and bend diameter have great effects on the microstructures. In order to obtain high-quality slurry, the microstructural evolution mechanism of the semi-solid slurry during the pouring process is analyzed, as shown in Fig. 9. Figure 9(a) shows the entire pouring process, and Figs. 9(b, c, d) show the early, middle and later stages of pouring process, respectively.

In the early stage of pouring process (Fig. 9(b)), after the melt is poured into the inner channel, the melt near the inner channel wall surface can be easily cooled to below its liquidus temperature, and a large number of primary α(Al) grains rapidly nucleate due to the chilling effect of the channel wall. In addition, the heterogeneous nucleation also occurs on the channel wall surface. It should be noted that the primary grains are easier to nucleate on the concave surface, which is due to the fact that the channel concave surface has a larger radius of curvature than the convex surface [22]. Most of the primary grains flow away with the melt, while a part of the grains remain and accumulate on the inner wall surface. This explains the formation of the residual solidified shell. Actually, the nucleation is greatly affected by temperature gradient and concentration gradient in the melt during the early pouring process. A few

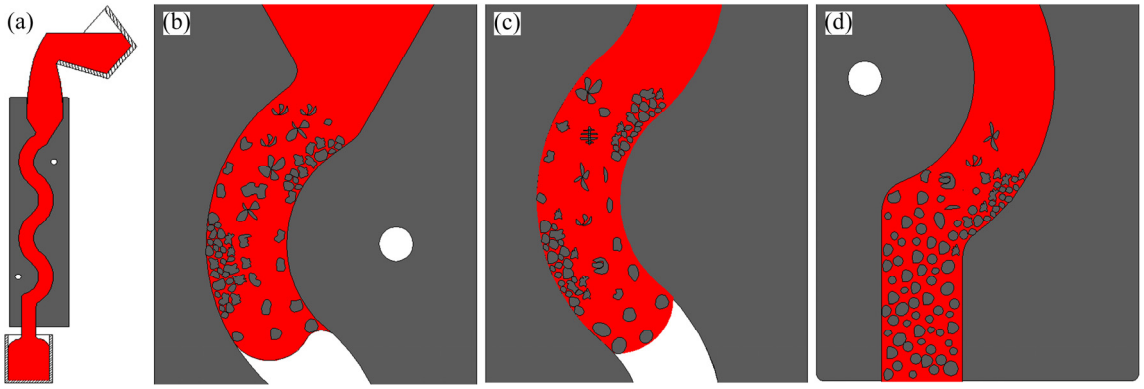

Fig. 9 Schematic diagram of microstructural evolution mechanism of semi-solid slurry: (a) Entire pouring process; (b) Early stage; (c) Middle stage; (d) Later stage

embryos grow into dendrites owing to the heterogeneity of temperature field and concentration field. And some embryos whose size does not reach the critical nucleation radius are remelted by a high-temperature melt.

In the middle stage of pouring process (Fig. 9(c)), the melt continuously moves forward under the action of gravity, and the "self-stirring" effect is strengthened after the melt passing through each bend. As a result, not only the heat transmission to the channel wall is improved, but also the structure fluctuation and energy fluctuation are generated, which promotes the nucleation. It should be pointed out that the density, temperature and solute concentration of the melt are constantly changed in the channel. And some dendrites are necked and fragmented due to the influence of convection, stress concentration and solute enrichment of the melt. The dendrite fragments gradually grow into free grains, and increase the nuclei number of the new primary α(Al) grains.

In the later stage of pouring process (Fig. 9(d)), before the melt flows out of the channel, the heat exchange between the melt and serpentine channel is greatly reduced. Therefore, the temperature field and concentration field in the melt become relatively uniform, and it is beneficial to the refinement and spheroidization of primary grains. This indicates that most of the primary grains will grow in a spherical manner. Finally, the slurry flows into a copper collection crucible. Under the action of gravity, the continuous injection accelerates the mutual stirring of the slurry, which further promotes the refinement and spheroidization of the primary grains.

As mentioned above, there are two kinds of nucleation mechanism of primary grains, one of which is forming directly from the alloy melt, such as chilling nucleation and heterogeneous nucleation, and the other is evolving from the fractured dendrite fragments. The heat exchange between the melt and the serpentine channel is increased by the "self-stirring" effect in the melt, and results in more homogeneous temperature field and concentration field. This is expected to further refine and spheroidize the primary grains, while inhibit the growth of dendrites.

In order to further understand the micro-structural evolution mechanism of the semi-solid slurry, the microstructures of solidified shell are analyzed, as shown in Fig. 10. Figures 10(a, b) show macroscopic morphologies of the whole and partially solidified shell, respectively. Figures 10(c, d, e) correspond to the microstructures of locations A,

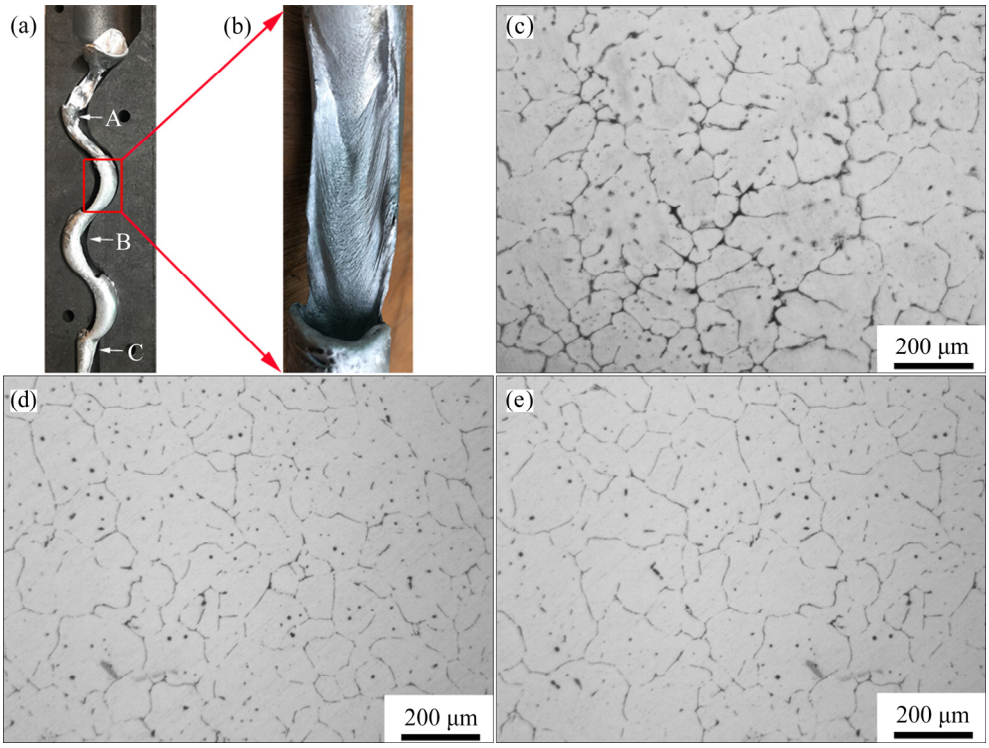

Fig. 10 Macroscopic morphology and microstructures of solidified shell: (a) Whole solidified shell; (b) Partially solidified shell; (c) Location A; (d) Location B; (e) Location C

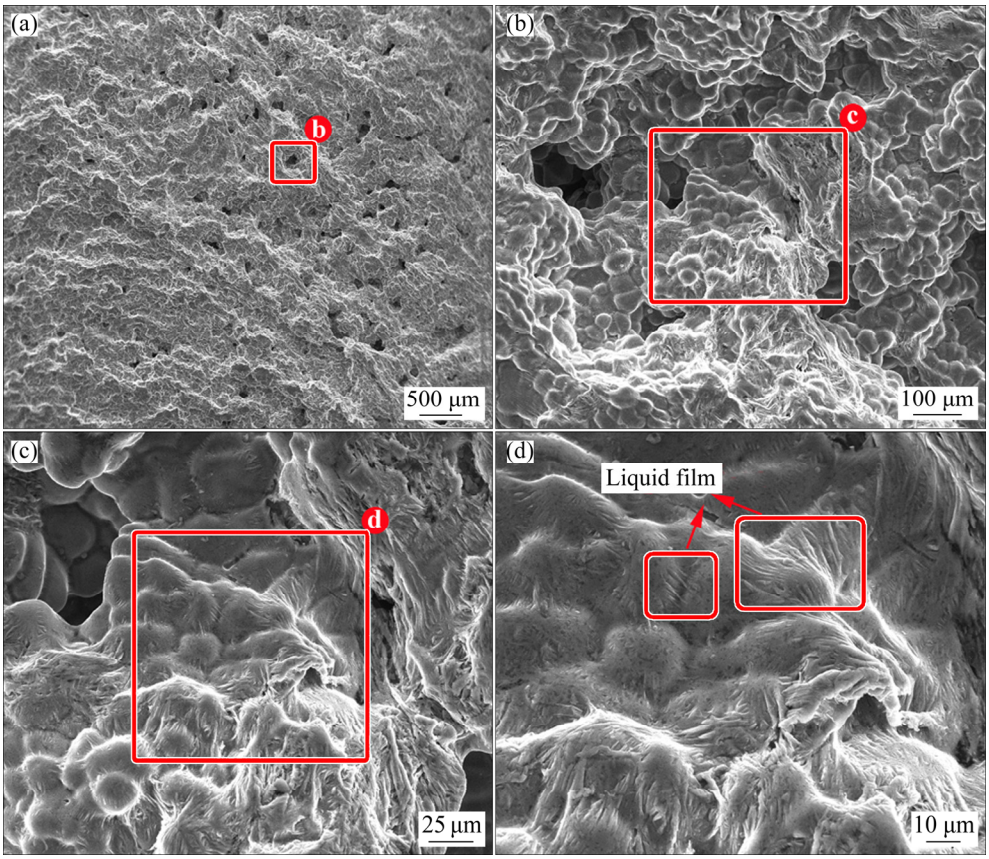

Fig. 11 Microscopic morphologies of solidified shell surface

B and C marked in Fig. 10(a), respectively. It can be clearly observed that the solidified shell surface has a river-like morphology (Fig. 10(b)). The primary α(Al) grains are mainly composed of coarser dendrites and a few dot-like dispersed phases (Fig. 10(c)). The dendrites are necked, fragmented and evolved into a rose-like morphology (Fig. 10(d)). A few near-spherical grains may be formed from dendrite fragments. In Fig. 10(e), the primary α(Al) grains are further spheroidized and evolved into a near-spherical morphology. It is observed that the grain size of solidified shell is relatively larger compared with that of the semi-solid slurry, but the grain roundness is relatively lower. In addition, the presence of dot-like dispersed phase in solidified shell is similar to the as-cast state. This is mainly related to the different cooling methods between the solidified shell and the semi-solid slurry. After the pouring process is completed, the solidified shell is slowly cooled to room temperature by air, and the dispersed phases can fully diffuse into the primary grains. However, the semi-solid slurry is rapidly water-cooled to retain the high-temperature microstructure, and the dispersed phases can be only distributed at the grain boundaries.

Figure 11 shows the microscopic morphology of the solidified shell surface. The solidified shell surface is scoured to be a river-like morphology with some potholes (Fig. 11(a)). And some near-spherical grains are distributed around the potholes (Fig. 11(b)). This indicates that the potholes are probably caused by the melt scoured away from part of the grains. Figures 11(c, d) show some filamentous liquid films on the grain surface [23,24]. The filamentous liquid films are formed by the shrinkage of the melt during solidification process. A few fine liquid films extend outward under the action of internal stress and solidify into hair-like morphologies (Fig. 11(d)).

5 Conclusions

(1) Semi-solid 6061 aluminum alloy slurry is successfully prepared by the SCP process. The microstructures of slurry are significantly refined and spheroidized compared with those of traditional permanent casting.

(2) The average grain diameter of primary α(Al) grains gradually increases with increasing pouring temperature, while the average shape factor gradually decreases. Under the same pouring conditions, the nucleation rate of primary α(Al) grains can be effectively increased by increasing the bend number and decreasing the bend diameter.

(3) The best quality semi-solid slurry can be obtained with pouring temperature of 660 °C, bend number of 6 and bend diameter of 20 mm. In this case, the average grain diameter of primary α(Al) grains is (56.08±22.71) μm, and the average shape factor is 0.73±0.14.

(4) The temperature field and concentration field tend to be uniform due to the "self-stirring" effect in the melt, which inhibits the growth of dendrites and promotes the spheroidization of primary grains.

References

[1] WANG Na, ZHOU Zhi-min, LU Gui-min. Microstructural evolution of 6061 alloy during isothermal heat treatment [J]. Journal of Materials Science & Technology, 2011, 27(1): 8−14.

[2] NEJADSEYFI O, SHOKUHFAR A, DABIRI A, AZIMI A. Combining equal-channel angular pressing and heat treatment to obtain enhanced corrosion resistance in 6061 aluminum alloy [J]. Journal of Alloys and Compounds, 2015, 648: 912−918.

[3] SHOKUHFAR A, NEJADSEYFI O. A comparison of the effects of severe plastic deformation and heat treatment on the tensile properties and impact toughness of aluminum alloy 6061 [J]. Materials Science and Engineering A, 2014, 594: 140−148.

[4] CHEN Xing-rui, JIA Yong-hui, LIAO Qi-yu, JIA Wei-tao, LE Qi-chi, NING Shao-chen, YU Fu-xiao. The simultaneous application of variable frequency ultrasonic and low frequency electromagnetic fields in semi continuous casting of AZ80 magnesium alloy [J]. Journal of Alloys and Compounds, 2019, 774: 710−720.

[5] MOUSTAFA E B, MOSLEH A O. Effect of (Ti−B) modifier elements and FSP on 5052 aluminum alloy [J]. Journal of Alloys and Compounds, 2020, 823. DOI:10.1016/j.jallcom.2020.153745.

[6] JUNG J G, AHN T Y, CHO Y H, KIM S H, LEE J M. Synergistic effect of ultrasonic melt treatment and fast cooling on the refinement of primary Si in a hypereutectic Al−Si alloy [J]. Acta Materialia, 2018, 144: 31−40.

[7] GUO Hong-min, YANG Xiang-jie, LUO Xue-quan. Formation of grain refined and non-dendritic microstructure of an aluminum alloy under angular oscillation [J]. Journal of Alloys and Compounds, 2009, 482(1/2): 412−415.

[8] FLEMINGS M C. Behavior of metal alloys in the semisolid state [J]. Metallurgical Transactions B, 1991, 22(3): 269−293.

[9] JIANG Ju-fu, WANG Ying. Microstructure and mechanical properties of the semisolid slurries and rheoformed component of nano-sized SiC/7075 aluminum matrix composite prepared by ultrasonic-assisted semisolid stirring [J]. Materials Science and Engineering A, 2015, 639: 350−358.

[10] CHANG Zhi-yu, SU Ning, WU Yu-juan, LAN Qiao, PENG Li-ming, DING Wen-jiang. Semisolid rheoforming of magnesium alloys: A review [J]. Materials & Design, 2020, 195. DOI: 10.1016/j.matdes.2020.108990.

[11] KUMAR S D, MANDAL A, CHAKRABORTY M. On the age hardening behavior of thixoformed A356−5TiB_2 in-situ composite [J]. Materials Science and Engineering A, 2015, 636: 254−262.

[12] MATHEW J, MANDAL A, KUMAR S D, BAJPAI S, CHAKRABORTY M, WEST G D, SRIRANGAM P. Effect of semi-solid forging on microstructure and mechanical properties of in-situ cast Al−Cu−TiB_2 composites [J]. Journal of Alloys and Compounds, 2017, 712: 460−467.

[13] WANG Cun-long, CHEN An-tao, ZHANG Liang, LIU Wen-cai, WU Guo-hua, DING Wen-jiang. Preparation of an Mg−Gd−Zn alloy semisolid slurry by low frequency electromagnetic stirring [J]. Materials & Design, 2015, 84: 53−63.

[14] FAN Ling-ling, ZHOU Ming-yang, ZHANG Yu-wenxi, TANG Qi, QUAN Gao-feng, LIU Bing. The semi-solid microstructural evolution and coarsening kinetics of AZ80−0.2Y−0.15Ca magnesium alloy [J]. Materials Characterization, 2019, 154: 116−126.

[15] QI Ming-fan, KANG Yong-lin, LI Jing-yuan, WULABIEKE Z, XU Yu-zhao, LI Yang-de, LIU Ai-sen, CHEN Jun-chen. Microstructures refinement and mechanical properties enhancement of aluminum and magnesium alloys by combining distributary-confluence channel process for semisolid slurry preparation with high pressure die-casting [J]. Journal of Materials Processing Technology, 2020, 285. DOI: 10.1016/j.jmatprotec.2020.116800.

[16] CHEN Zheng-zhou, MAO Wei-min, WU Zong-chuang. Influence of serpentine channel pouring process parameters on semi-solid A356 aluminum alloy slurry [J]. Transactions of Nonferrous Metals Society of China, 2011, 21(5): 985−990.

[17] LIU Zhi-yong, MAO Wei-min, WANG Wei-pan, ZHENG Zhi-kai. Preparation of semi-solid A380 aluminum alloy slurry by serpentine channel [J]. Transactions of Nonferrous Metals Society of China, 2015, 25(5): 1419−1426.

[18] JIANG Ju-fu, WANG Ying, XIAO Guan-fei, NIE Xi. Comparison of microstructural evolution of 7075 aluminum alloy fabricated by SIMA and RAP [J]. Journal of Materials Processing Technology, 2016, 238: 361−372.

[19] HU X G, ZHU Q, LU H X, ZHANG F, LI D Q, MIDSON S P. Microstructural evolution and thixoformability of semi-solid aluminum 319s alloy during re-melting [J]. Journal of Alloys and Compounds, 2015, 649: 204−210.

[20] WANG Yong-fei, ZHAO Sheng-dun, ZHAO Xu-zhe, ZHAO Yong-qiang. Effects of isothermal treatment parameters on the microstructure of semisolid alloys [J]. Materials Science and Technology, 2018, 34(1): 104−110.

[21] ZHU Wen-zhi, MAO Wei-min, TU Qin. Preparation of

semi-solid 7075 aluminum alloy slurry by serpentine pouring channel [J]. Transactions of Nonferrous Metals Society of China, 2014, 24(4): 954−960.

[22] LI Xiang-ming, LIU Qing-hui. Heterogenous nucleation in a cave with an apex and iso-curvature lateral surface [J]. Journal of Crystal Growth, 2015, 426: 66−70.

[23] WANG Zhi, LI Yi-zhou, WANG Feng, HUANG Yuan-ding, SONG Jiang-feng, MAO Ping-li, LIU Zheng. Hot tearing susceptibility of Mg−*x*Zn−2Y alloys [J]. Transactions of Nonferrous Metals Society of China, 2016, 26(12): 3115−3122.

[24] XU Rong-fu, ZHENG Hong-liang, LUO Jie, DING Su-pei, ZHANG San-ping, TIAN Xue-lei. Role of tensile forces in hot tearing formation of cast Al−Si alloy [J]. Transactions of Nonferrous Metals Society of China, 2014, 24(7): 2203−2207.

采用蛇形通道浇注法制备半固态 6061 铝合金浆料

李乃拥，毛卫民，耿晓鑫

北京科技大学 材料科学与工程学院，北京 100083

摘　要：采用蛇形通道浇注工艺制备半固态 6061 铝合金浆料。研究浇注温度、弯道数量和弯道内径对显微组织的影响，并分析半固态浆料在浇注过程中的显微组织演变机理。结果表明：控制浇注温度在液相线附近可以细化晶粒、提高晶粒圆整度，并且增加弯道数量和降低弯道内径可以有效增加初生 α(Al) 晶粒的形核率。初生晶粒不仅由合金熔体受激冷形核和异质形核作用直接形成，而且还由断裂的枝晶碎片演化而来；同时，熔体中的“自搅拌”效应可提高熔体与蛇形通道之间的热交换，也促进初生 α(Al)晶粒的细化和球化。

关键词：6061 铝合金；半固态浆料；蛇形通道；显微组织演变

(Edited by Bing YANG)